GROUND COUPLED SOLAR HEAT PUMPS: ANALYSIS OF FOUR OPTIONS

J. W. Andrews

Prepared for presentation at the ASME Solar Energy Division Conference, The American Society of Mechanical Engineers, Reno, Nevada, April 27 - May 1, 1981

DEPARTMENT OF ENERGY AND ENVIRONMENT

BROOKHAVEN NATIONAL LABORATORY
UPTON, NEW YORK 11973

DISCLAIMER

BNL-29007

GROUND COUPLED SOLAR HEAT PUMPS: ANALYSIS OF FOUR OPTIONS

J. W. Andrews

Prepared for presentation at the ASME Solar Energy Division Conference
The American Society of Mechanical Engineers
Reno, Nevada, April 27 - May 1, 1981

DEPARTMENT OF ENERGY AND ENVIRONMENT
BROOKHAVEN NATIONAL LABORATORY
ASSOCIATED UNIVERSITIES, INC.

Under Contract No. DE-AC02-76CH00016 with the
U.S. Department of Energy

ABSTRACT

Heat pump systems which utilize both solar energy and energy withdrawn from the ground are analyzed using a simplified procedure which optimizes the solar storage temperature on a monthly basis. Four ways of introducing collected solar energy to the system are optimized and compared. These include use of actively collected thermal input to the heat pump; use of collected solar energy to heat the load directly (two different ways); and use of a passive option to reduce the effective heating load.

NOMENCLATURE

A	collector area, m^2
b	ground heat transfer coefficient, kJ/hr-°C-m
COP	coefficient of performance
D	number of °C-days
E	energy, kJ
F_R	collector heat removal factor
h	number of hours with sun
I	insolation rate, $kJ/hr-m^2$
N	number of days in month
Q	incremental heat loss, kJ
S	incident insolation per unit area of tilted surface, kJ/m^2
T	temperature, °K
U	heat loss coefficient, $kJ/hr-°C-m^2$
U_L	collector heat loss factor, $kJ/hr-°C-m^2$
α	absorber plate absorptivity
γ	fraction of Carnot efficiency
η	collector efficiency
τ	effective glazing transmissivity

Subscripts

a	ambient
c	collected (energy)
c	COP parameter (temperature)
f	far-field
g	ground-source (energy)
l	load
m	maximum
p	purchased
s	solar-source (energy)
s	day-night swing (temperature)
x	ground-source (temperature)

*Work performed under the auspices of the Active Solar Heating and Cooling Division, United States Department of Energy, Contract No. DE-AC02-7600016.

INTRODUCTION

The objective of this study was to evaluate the desirability of adding solar energy input to heat pump systems which use the ground as their primary heat source for space and water heating and heat sink for cooling. Four ways of collecting and using solar energy in such systems were identified:

1. Actively collected solar energy and heat removed from the ground are both used as sources of thermal energy to the heat pump.
2. Actively collected solar energy is delivered directly to the building load, with the ground coupled heat pump as backup.
3. Actively collected solar energy preheats the return air stream from the building, and the heat pump raises the air temperature further (if necessary) to the value required for comfort.
4. Solar energy collected via direct-gain passive design is used to reduce the building load required to be met by the ground coupled heat pump.

In each of the three active solar options the heat pump produces hot water to the extent that solar energy is inadequate. In the passive option all of the hot water is produced via the heat pump.

The study was undertaken for three cities (Atlanta, New York, and Madison) providing a range of heating season environments from mild to severe. Since the collectors are not used for cooling in the systems under consideration, cooling performance is independent of the collector type and it was therefore not necessary to include cooling in the model in order to compare different collectors and

operating modes. It was assumed, however, that reject heat from air conditioning was used to heat water during the cooling season, which was taken to equal three months in New York and five months in Atlanta. In Madison a heating-only heat pump was assumed.

In the three modes which involve active solar subsystems the solar energy is stored in an insulated tank, rather than in the ground, and the ground is used solely as a heat source and sink rather than as a storage element. The ground coupling heat exchanger configuration chosen - a horizontal plane serpentine coil of buried plastic pipe - is particularly suited for use as a source or sink but is not capable of long-term energy storage (1). Therefore it should be carefully noted that the results of this paper apply only to such systems and not to systems in which in-ground storage is attempted.

APPROACH

The approach taken in this study has been reported previously (2). It was desired to develop an analytical model of ground coupled solar heat pump systems which could be used to compare the solar operating modes described above. Two desirable characteristics have been identified for such an approach. They are:

1. The approach should be simple enough so that all of the assumptions used in the study can be stated explicitly in a paper of moderate length.
2. The approach must be capable of optimizing each operating mode, so that there will be no need to worry that one mode performed better than another merely because its operating parameters were closer to their optimum values.

For each of the active solar options, the optimum storage temperature was found, for each month, via a computer search over the entire allowed range of temperatures. This procedure, strictly speaking, assumes a constant storage temperature throughout any month, and it further assumes that this storage temperature is subject to control. Practically, the constant storage temperature is intended to represent the effect of an oscillating storage temperature which cycles above and below the assumed constant temperature. Since the result of the computer search is an optimum storage temperature, excursions from this value will represent suboptimal operation and to this extent the actual performance of the solar system will be somewhat poorer than predicted. Losses from storage are neglected, as is the pumping power needed to pass fluid through the collectors. The inlet temperature to the collector subsystem and the inlet temperature to the heat pump are both assumed equal to the (uniform) storage temperature. Collector and heat pump performance are expressed in terms of these inlet temperatures. Thus there is only one quantity, the storage temperature, which needs to be varied in the optimization process, for any given collector area and ground coupling heat exchanger size. Controllability of the storage temperature in practice can be effected be controlling, on a monthly basis, the minimum storage temperature below which the system turns to the ground as the alternate heat source. By setting this minimum the right amount below the optimum, the average storage temperature during any month can be tuned to equal the optimum.

COMPONENT MODELING

Active Collector

Collector performance is modeled via the usual Hottel-Whillier straight-line graph of efficiency vs $(T - T_a)/I$, where T is the collector inlet temperature, T_a is the ambient temperature, and I is the insolation rate. The performance curve is represented by two parameters, the vertical and horizontal intercepts of the collector efficiency curve. The vertical intercept is equal fo $F_R\tau\alpha$, where F_R is the collector heat removal factor, τ is the effective glazing transmissivity, and α is the absorber plate absorptivity, while the horizontal intercept is equal to $\tau\alpha/U_L$, where U_L is the collector heat loss factor (3).

Two collector types were studied. The first, called in this paper the "high performance collector", is characterized by a vertical intercept $F_R\tau\alpha$ of 0.7 and a horizontal intercept $\tau\alpha/U_L$ equal to 0.04 $^oC\text{-hr-m}^2/kJ$. This corresponds approximately to a single glazed collector with a selective surface absorber. The second collector, called here the "heat pump collector", is characterized by $F_R\tau\alpha = 0.7$ and $\tau\alpha/U_L = 0.02\,^oC\text{-hr-m}^2/kJ$. This corresponds approximately to a trickle-type collector such as the Thomason Solaris™ or to a single-glazed extruded plastic collector such as the FAFCO IV™ which is being marketed for use with heat pumps.

The intensity of the insolation striking the collector during daylight hours is taken to be a random variable with a constant probability density for insolation values between 0 and I_m. That portion of received insolation falling with intensity greater than $(T - T_a)/(\tau\alpha/U_L)$ can be partially collected with efficiency increasing with increasing I. The lower-intensity insolation is lost completely. It can be shown (see Appendix) that under these assumptions the total energy that can be collected at temperature T is given by

$$E_c = SAF_R\tau\alpha\left(\frac{T_m-T}{T_m-T_a}\right)^2 \qquad (1)$$

where S is the received insolation on a unit area of collector, A is the collector area, and T_m is the maximum stagnation temperature $T_a + I_m\,\tau\alpha/U_L$.

In order to test the adequacy of (1) to represent the operation of the collectors, comparisons were made for each of the three cities of monthly and annual solar fractions computed using (1) with those obtained using f-chart (4,5). For this comparison a collector operating temperature of 40°C was assumed in (1), and I_m was set equal to 3410 $kJ/m^2\text{-hr}$. Collector tilt was set at latitude plus 10°. Results of the comparison are shown in Tables 1 through 3 for the high performance collector. For the heat pump collector the degree of agreement between (1) and f-chart was comparable to that seen in Tables 1 through 3, execpt for Madison where (1) gave yearly solar fractions about 25% below those of f-chart.

Passive Collector

It was desired to compare a simple passive design option, such as direct gain, with the active options for use with ground coupling. A simple model was constructed of a direct-gain system with

Table 1

Comparison of Solar Fractions (f) Obtained Using Eq. 1 with Those of f-chart (f*).
Location: Madison, Wisconsin

Month	Heating & Hot Water Load (GJ)	Insolation on Tilted Collector (GJ/m^2)	Average Ambient Temperature (°C)	A = 20 m^2		A = 40 m^2		A = 60 m^2		Other Monthly Data	
				f	f*	f	f*	f	f*	Far-Field Temperature (°C)	Insolation on Vertical (GJ/m^2)
Jan.	21.01	0.405	-8.1	0.11	0.14	0.22	0.27	0.34	0.37	3.3	0.386
Feb.	18.34	0.415	-6.0	0.14	0.19	0.27	0.35	0.41	0.49	0.8	0.362
Mar.	15.89	0.551	-0.2	0.23	0.28	0.47	0.50	0.70	0.67	0.1	0.422
Apr.	8.91	0.483	7.9	0.44	0.42	0.87	0.69	1.00	0.85	1.6	0.309
May	4.48	0.510	13.8	1.00	0.72	1.00	0.95	1.00	1.00	4.9	0.288
June	1.71	0.532	19.4	1.00	1.00	1.00	1.00	1.00	1.00	9.2	0.279
July	1.71	0.573	21.8	1.00	1.00	1.00	1.00	1.00	1.00	13.2	0.306
Aug.	1.71	0.562	20.9	1.00	1.00	1.00	1.00	1.00	1.00	15.9	0.338
Sept.	2.60	0.574	16.0	1.00	1.00	1.00	1.00	1.00	1.00	16.6	0.412
Oct.	6.82	0.535	10.5	0.67	0.57	1.00	0.85	1.00	0.97	15.0	0.453
Nov.	13.35	0.350	1.9	0.19	0.19	0.37	0.35	0.56	0.48	11.6	0.325
Dec.	18.99	0.383	-5.2	0.13	0.15	0.25	0.27	0.38	0.38	7.4	0.374
Year	115.52			0.30	0.30	0.47	0.47	0.59	0.58		

Table 2
Comparison of Solar Fractions (f) Obtained Using Eq. 1 with Those of f-Chart (f*).
Location: New York, New York

Month	Heating & Hot Water Load (GJ)	Insolation on Tilted Collector (GJ/m^2)	Average Ambient Temperature (°C)	A = 20 m^2		A = 30 m^2		A = 40 m^2		Other Monthly Data	
				f	f*	f	f*	f	f*	Far-Field Temperature (°C)	Insolation on Vertical (GJ/m^2)
Jan.	15.36	0.333	0.1	0.15	0.15	0.23	0.21	0.30	0.28	5.7	0.309
Feb.	14.04	0.360	0.8	0.18	0.21	0.27	0.30	0.36	0.38	3.4	0.305
Mar.	11.86	0.487	5.1	0.32	0.32	0.48	0.45	0.64	0.56	3.2	0.360
Apr.	6.63	0.456	11.2	0.60	0.51	0.90	0.67	1.00	0.79	5.3	0.280
May	2.03	0.492	16.8	1.00	0.97	1.00	1.00	1.00	1.00	9.0	0.264
June	1.71	0.512	22.0	1.00	1.00	1.00	1.00	1.00	1.00	13.6	0.255
July	1.71	0.538	24.8	1.00	1.00	1.00	1.00	1.00	1.00	17.4	0.274
Aug.	1.71	0.583	23.8	1.00	1.00	1.00	1.00	1.00	1.00	19.9	0.331
Sept.	1.71	0.507	20.2	1.00	1.00	1.00	1.00	1.00	1.00	20.1	0.350
Oct.	3.58	0.482	14.8	1.00	0.78	1.00	0.92	1.00	1.00	18.0	0.397
Nov.	8.43	0.339	8.6	0.33	0.29	0.50	0.40	0.66	0.50	14.1	0.308
Dec.	14.01	0.308	1.9	0.16	0.14	0.24	0.21	0.32	0.27	9.7	0.292
Year	82.78			0.36	0.34	0.47	0.43	0.56	0.50		

Table 3

Comparison of Solar Fractions (f) Obtained Using Eq. 1 with Those of f-Chart (f*).
Location: Atlanta, Georgia

Month	Heating & Hot Water Load (GJ)	Insolation on Tilted Collector (GJ/m^2)	Average Ambient Temperature (°C)	A = 10 m^2 f	A = 10 m^2 f*	A = 20 m^2 f	A = 20 m^2 f*	A = 30 m^2 f	A = 30 m^2 f*	Other Monthly Data Far-Field Temperature (°C)	Other Monthly Data Insolation on Vertical (GJ/m^2)
Jan.	10.63	0.468	5.8	0.17	0.18	0.34	0.34	0.52	0.47	12.1	0.420
Feb.	8.83	0.448	7.2	0.20	0.23	0.41	0.42	0.61	0.58	10.4	0.358
Mar.	7.18	0.557	10.6	0.33	0.33	0.67	0.57	1.00	0.74	10.3	0.375
Apr.	2.57	0.577	16.2	1.00	0.77	1.00	1.00	1.00	1.00	11.7	0.301
May	1.71	0.577	20.6	1.00	0.93	1.00	1.00	1.00	1.00	14.4	0.252
June	1.71	0.544	24.2	1.00	0.93	1.00	1.00	1.00	1.00	17.7	0.221
July	1.71	0.562	25.6	1.00	0.93	1.00	1.00	1.00	1.00	20.5	0.237
Aug.	1.71	0.586	25.3	1.00	0.96	1.00	1.00	1.00	1.00	22.3	0.284
Sept.	1.71	0.552	22.4	1.00	0.93	1.00	1.00	1.00	1.00	22.4	0.341
Oct.	2.13	0.597	16.9	1.00	0.86	1.00	1.00	1.00	1.00	20.9	0.460
Nov.	7.05	0.521	10.8	0.32	0.32	0.64	0.56	0.95	0.73	18.1	0.461
Dec.	10.83	0.427	6.4	0.16	0.16	0.31	0.30	0.47	0.42	14.9	0.393
Year	57.77			0.40	0.38	0.57	0.55	0.75	0.66		

movable insulation which is set in place at night to reduce heat loss from the building. The net thermal gain from the vertical south-facing aperture is calculated as the difference between the thermal gain due to incident radiation and the incremental thermal losses due to the fact that the direct-gain aperture replaced wall area having a different (usually lower) net heat loss coefficient.

The radiation gain was simply taken to equal 65% of the radiation incident on the vertical aperture area, while the monthly incremental thermal losses Q were taken to equal

$$Q = 12D\,(U_n + U_d - 2U_o) - 3.6\,NT_s\,(U_d - U_n) \quad (2)$$

where N is the number of days in the month, D is the number of heating °C-days, T_s is the mean day-night temperature swing (typically 10°C), U_d is the heat loss coefficient of the direct-gain aperture during the day, U_n is the heat loss coefficient at night, with movable insulation in place, and U_o is the heat loss coefficient of the wall which is replaced. Values used in the analysis were U_d, U_n, and U_o equal to 10, 2, and 1 kJ/m^2-hr-°C, respectively. The second term on the right-hand side of (2) takes into account the fact that the ambient temperature at night, when the movable insulation is in place, is lower than during the day. Hence the thermal losses are less than would be expected from a simple averaging of the day and night U-values, as represented by the first term. Annual energy savings from a direct-gain passive system with night insulation, calculated using the above procedure, were compared with results from a more detailed analysis (6). Results of this comparison are shown in Figure 1. Monthly incident insolation on a vertical surface, used in (2), is shown in the last column in Tables 1 through 3.

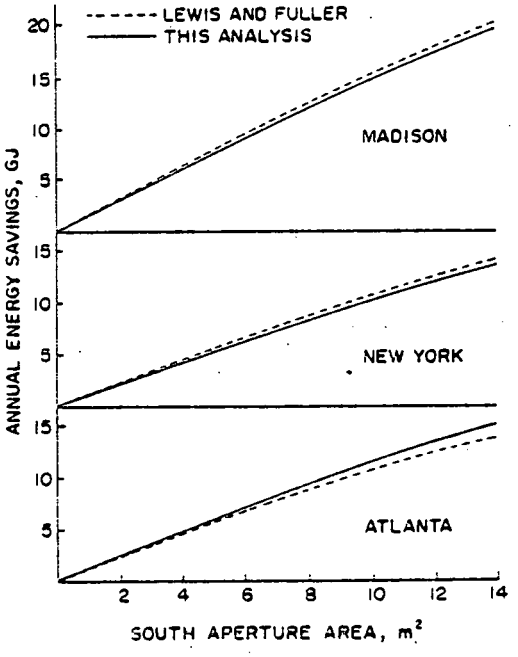

Figure 1. Annual Energy Savings from Direct Gain with Night Insulation.

Heat Pump and Direct Heating Coil

The coefficient of performance, COP, of the heat pump, whether utilizing the solar source or the ground source, is modeled (7) as a constant fraction γ of Carnot:

$$COP = \frac{\gamma T_c}{T_c - T} \quad . \qquad (3)$$

Because of the form of (3), all temperatures must be represented in absolute units in what follows. The parameters γ and T_c are set to give desired COP values at any two temperatures. In this study γ was set at 0.498 and $T_c = 335^\circ K$, consistent with a heating COP of 2.5 at a source temperature of $-5^\circ C$ (8) and 4.0 at $20^\circ C$ (9).

Direct heating from solar, bypassing the heat pump, was assumed to be possible at source temperatures of $40^\circ C$ and above, with a coefficient of performance increasing by 0.7 for each $^\circ C$ difference between the source temperature and the room temperature of $20^\circ C$ or $293^\circ K$ (10), or

$$COP = 0.7\ (T - 293) \quad . \qquad (4)$$

Thus the COP for direct heating is 14 at $40^\circ C$, while the heat pump COP at the same temperature is 7.6. The performance curves for the heat pump and direct heating are shown in Figure 2.

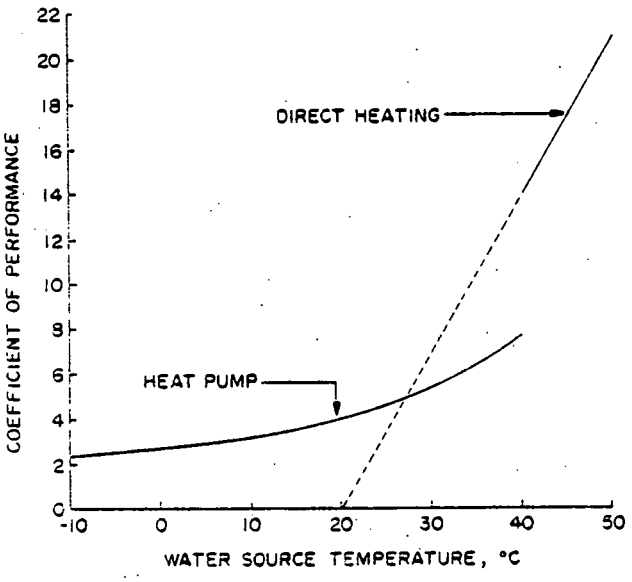

Figure 2. Heat Pump and Direct Heating COP vs Water Source Temperature

The heat pump performance curve differs from typical data obtained with current-generation single-speed water source heat pumps, whose coefficients of performance do not rise so steeply with source temperature in the 20 to $40^\circ C$ range. One objective of the U. S. Department of Energy's solar assisted heat pump research and development program has been to produce a heat pump exhibiting performance such as represented by Figure 2. This objective is being pursued primarily through the use of variable-capacity compressors and appropriately sized heat exchangers. Progress of this development is discussed in (11).

It is now possible to calculate the total energy E_s delivered by the solar source heat pump or direct-heating coil, as well as the purchased energy E_{ps} needed to operate either device.

For the solar source heat pump the delivered energy is given by

$$E_s = \frac{COP}{COP - 1} E_c \qquad (5)$$

$$= \frac{\gamma E_o (T_m - T)^2}{T_c (T - T_d)} \qquad (6)$$

where $E_o = SAF_R \tau\alpha\ T_c^2/(T_m - T_a)^2$, and $T_d = (1 - \gamma)T_c$.

The purchased energy required to operate the heat pump is given by

$$E_{ps} = \frac{E_s}{COP} \qquad (7)$$

$$= \frac{E_o(T_c - T)(T_m - T)^2}{T_c^2(T - T_d)} \quad . \qquad (8)$$

For the direct heating coil, (4) rather than (3) is substituted into (5) and (7) to obtain E_s and E_{ps}.

Ground-Coupled Heat Exchanger

It is assumed that the energy E_g extracted from the ground is proportional to the difference between the temperature T_x at which heat is extracted and the temperature T_f of undisturbed ground at the same depth at the same time of the year, or far-field temperature:

$$E_g = (T_f - T_x)\ b \quad . \qquad (9)$$

The constant b is a product of the inherent heat transfer capability of the ground coupling device, in kJ/hr-$^\circ$C-m for linear pipes or kJ/hr-$^\circ$C-m^2 for tanks or planar devices; the size of the device in linear or square meters; and the number of hours in the time period, e.g. 720 hr/month. The COP of the heat pump using the ground as an energy source is the ratio of the energy E_x supplied by the ground source heat pump to the purchased energy E_{px} needed to operate the heat pump:

$$\frac{E_x}{E_{px}} = \frac{\gamma T_c}{T_c - T_x} \quad . \qquad (10)$$

Two energy balance equations can be written, the one on the ground-source heat pump given by

$$E_x = E_g + E_{px} \qquad (11)$$

and the one on the load given by

$$E_x = E_\ell - E_s \qquad (12)$$

where E_ℓ is the heating and hot water load and E_s is the energy supplied by the solar source heat pump or direct heating coil.

Solving (9) through (12) for E_{px} (eliminating E_x, E_g, and T_x) yields

$$E_{px} = \frac{(E - E_s)(E - E_s + bT_c - bT_f)}{bT_c + E - E_s} \quad (13)$$

Values of the far-field temperature T_f used in this analysis were calculated (12) for a depth of 1.5 m and a soil thermal diffusivity of 0.00372 m^2/hr. They are given in the second-last column of Tables 1 through 3.

Load

The heating loads were designed to match the requirements of ASHRAE Standard 90-75 (13) for a single-floor residence of 140 m^2 floor area. Thermal losses through the walls, ceiling, and floor were considered, as well as losses due to infiltration of outside air. The overall heat loss factor or UA value required by the standard is a function of the number of annual heating degree days. The only modification to the standard was that the requirement given for more than 4000 °F-days (2222 °C-days) was used throughout the range of heating climates. The ASHRAE 90-75 standard for warmer climates is much less stringent and it was decided to adhere to the more stringent standards in all climates. The resulting UA value for the structure was

$$UA = 1353 - 0.0365D \quad kJ/hr-°C \quad (14)$$

where D is the number of °C-days in the annual heating season. Monthly heating loads were then determined by multiplying the UA value by 24 times the number of heating degree days in the month. Internal gains of 53,000 kJ/day were subtracted from this load. If the internal gains exceeded the heating load as calculated from the UA value, the heating load was set to zero.

The hot water load was set equal to 56,000 kJ per day. The hot water load could be met either by the heat pump or the active collectors, but not by the passive structure.

SYSTEM OPTIMIZATION

Optimization of the system operating temperature (storage temperature) is carried out separately for each of three active options. For the passive option, the reduced space heating load resulting after passive gains are subtracted is met by the ground coupled heat pump. The search for an optimum temperature is carried out in 0.2 °C steps over the allowed range. For each temperature the purchased energy values E_{ps} (to operate the solar source subsystem) and E_{px} (to operate the ground source subsystem) are added, and the storage temperature yielding the minimum amount of purchased energy is selected as the optimum. The system optimization for each of four options is now discussed.

Series/Direct Heating

In this option solar energy is passed through the heat pump if the storage temperature is below 40 °C, while for storage temperatures above 40 °C the solar energy is passed to the load directly. Note that the same heat pump is used to process both solar and ground source heat. The temperature range over which the search for optimum is carried out is from -20 °C up to the stagnation temperature of the collector for ten collector areas and eight values of the ground coupling constant b in (9), resulting in 80 separate operating conditions. For each operating condition the fraction F of nonpurchased energy (ground plus solar) is calculated. By interpolation within this 8 X 10 matrix, curves of constant F can be plotted against collector area A and ground coupling field heat transfer factor b. Such curves are shown for the series/direct heating option by the solid lines in Figures 3 through 8 for each combination of collector type (high performance collector, heat pump collector) and location.

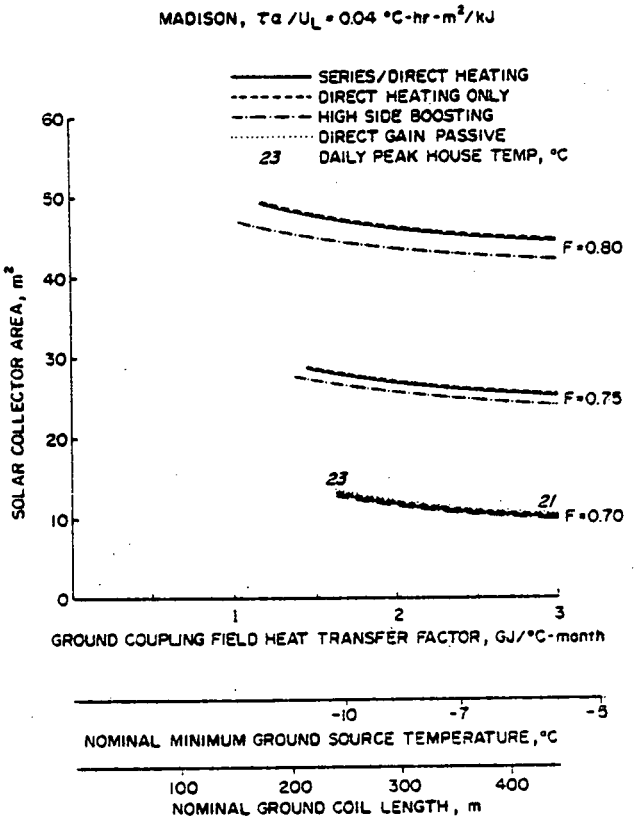

Figure 3. Solar Collector Areas and Ground Coupling Coil Capacities Required to Produce a Fraction F of Nonpurchased Energy Use. High Performance Collector in Madison.

Direct Heating Only

This option was treated by restricting the range of temperatures included in the search for an optimum. The search was carried out only over temperatures exceeding 40 °C, thus ruling out use of the heat pump to process solar energy. Curves of constant fractions F of nonpurchased energy are given by the dashed lines in Figures 3 through 8. Since the set of possible operating conditions under this option is a proper subset of those allowed under the previous option, the direct heating only curves will always lie on or above those for series/direct heating.

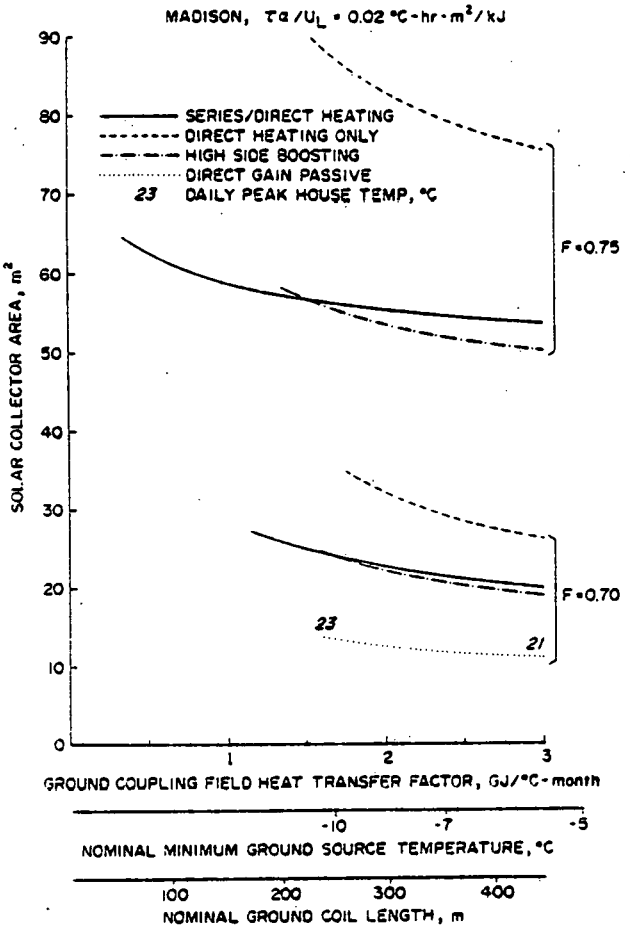

Figure 4. Solar Collector Areas and Ground Coupling Coil Capacities Required to Produce a Fraction F of Non-purchased Energy Use. Heat Pump Collector in Madison.

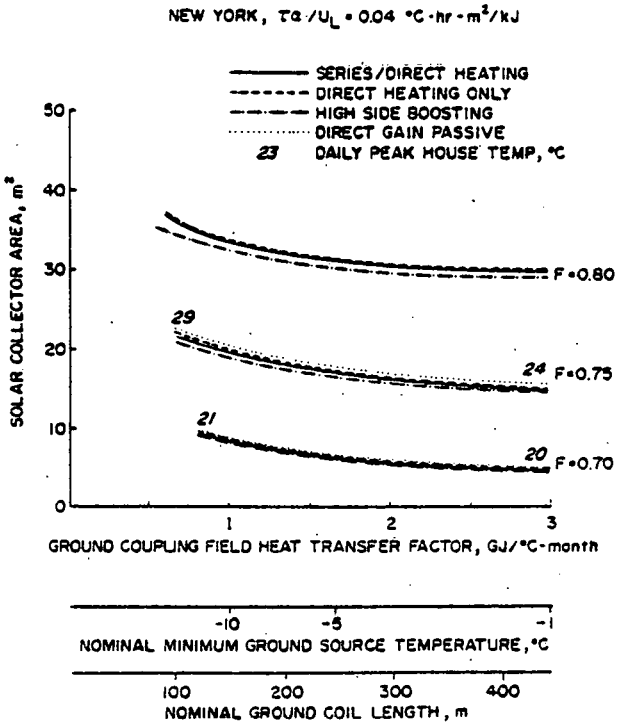

Figure 5. Solar Collector Areas and Ground Coupling Coil Capacities Required to Produce a Fraction F of Non-purchased Energy Use. High Performance Collector in New York

High Side Boosting

It has been suggested (14) that the optimal use of the collectors in a solar heat pump system is to preheat the return air stream from the building and then to use the heat pump to raise the air temperature further (if necessary) to the value required for delivery to the heated space. An approximate treatment of this option was made by allowing the search for the optimum temperature under the direct heating mode to extend below 40°C, with a COP as a function of temperature following the dashed line in Figure 2. This procedure involves at least two partially compensating inaccuracies. To the extent that the heat pump and the direct heating coil operate simultaneously, the fan power requirements are doubly counted, resulting in an underestimate of system performance. On the other hand, the heat pump condensing temperature tends to be higher for this option since the temperature of the preheated entering air stream is higher than for the other options. This will degrade heat pump COP somewhat, and this condition results in an overestimate of system performance. The extent to which these errors cancel has not been determined. The results for the high-side boosting option are given by the dash-dot lines in Figures 3 through 8.

Direct Gain Passive

For this option the reduction in heating load due to presence of the passive subsystem is computed on a monthly basis, and subtracted from the gross heating load to obtain a net heating load. If the potential gain from passive exceeds the gross heating load, the net heating load is set to zero. The hot water load is kept separate since it cannot be met by the passive structure.

The results for the direct gain passive option are given by the dotted lines in Figures 1 through 8. The passive results, of course, are not related to the active collector characteristics which are specified for the other three options; the same curve is given on both figures for each city to facilitate comparisons.

The maximum house temperature produced by the passsive subsystem was calculated using the procedure in Ref. 6. If it was not possible to achieve a given fraction of nonpurchased energy without heating the house above 26°C, the curve was not plotted.

SYSTEM COMPARISON

Inspection of Figures 3, 5, and 7 reveals that for the high performance collector it does not matter much which option is chosen, in terms of collector area. In the series/direct heating option, the optimization procedure always results in

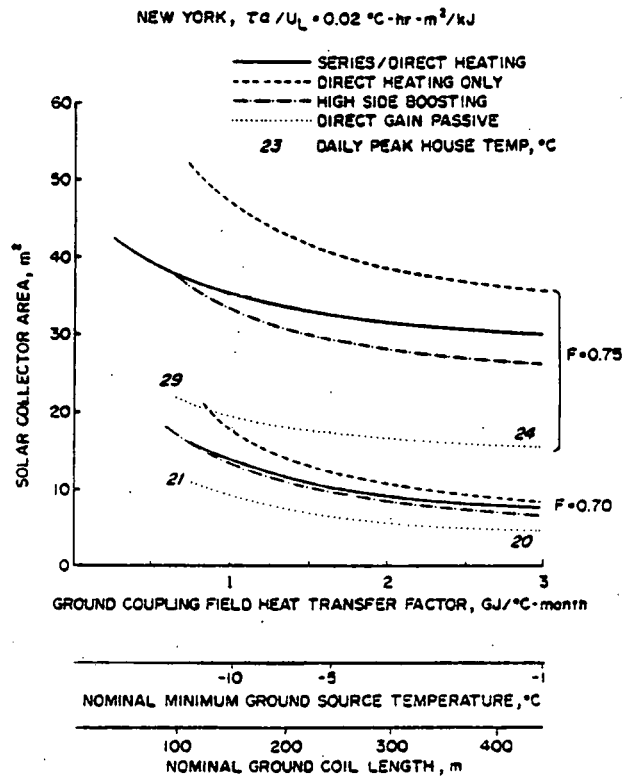

Figure 6. Solar Collector Areas and Ground Coupling Coil Capacities Required to Produce a Fraction F of Non-purchased Energy Use. Heat Pump Collector in New York.

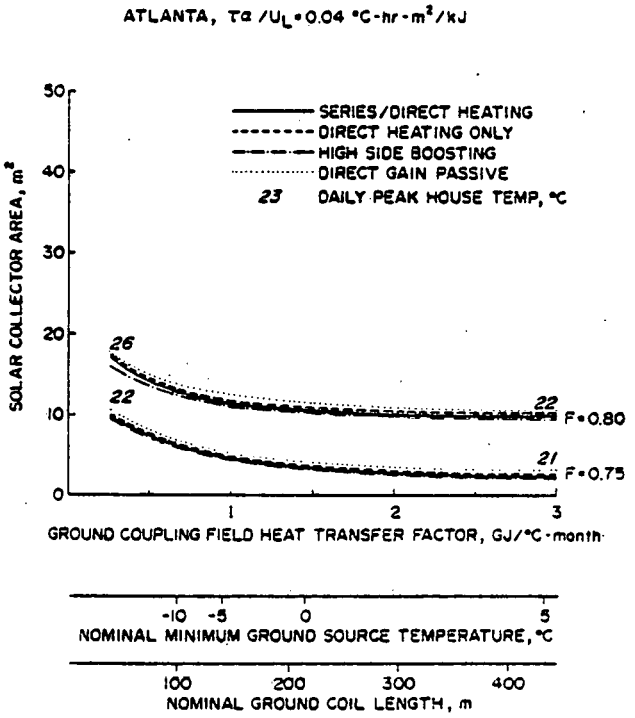

Figure 7. Solar Collector Areas and Ground Coupling Coil Capacities Required to Produce a Fraction F of Non-purchased Energy Use. High Performance Collector in Atlanta.

direct heating being chosen, so that no heat is processed through the heat pump and the series capability is not used. The enhancement in performance due to the lower operating temperatures in the boosting option is not large because the collector efficiency curve is relatively flat. The passive curves, although calculated via an entirely different procedure, lie very close to the active curves in all three cities. For the heat pump collector (Figures 4, 6, and 8), both the series/direct heating option and the boosting option result in significant performance enhancements over direct heating only. In the former option, the series mode is chosen in the colder months, with reversion to direct heating in spring and fall, the timing of the reversion depending on location and collector area. The optimum storage temperatures in the series mode ranged from 11 to 27°C in Madison, for $b \geq 2$ GJ/°C-month; 15 to 29°C in New York, for $b \geq 1.5$ GJ/°C-month; and 22 to 29°C in Atlanta, for $b \geq 1.0$ GJ/°C-month. These optimum temperatures are higher than the minimum source temperatures of ~5°C used in most simulations of series heat pump systems. The optimum temperatures are this high because the series mode competes with ground coupling as explained in (2); that is, because the ground source COP is itself relatively good, the series mode must have a significantly better COP in order for it to improve overall sytem performance. This requires a relatively high source temperature. But this reduces the amount of solar energy collected, which tends to defeat the purpose of the solar subsystem in the series mode.

ECONOMICS

Ground Coil

It was desired to relate both the ground coil and collector characteristics to real world capabilities and costs. In order to do this for the ground coil, it was first necessary to relate the ground coupling heat transfer coefficient b, expressed in GJ/°C-month (30 days), to an actual length of pipe in the ground. To do this, a heat transfer coefficient of 9.35 kJ/hr-°C-m (1.5 Btu/hr-°F-ft) was assumed for the pipe. This is conservative relative to published values (15, 1a). However, it must be understood that this value is a function of the characteristics of the soil and of whether coil is used more or less continuously or intermittently. For these reasons the term "nominal" is attached to the ground coupled coil lengths shown parallel to the horizontal axes of Figure 3 through 8. The curves in these figures extend leftward to a point where the minimum ground source temperature, assuming uniform input from the ground and the solar collectors, is -5°C. This is not a very good assumption and would result in grossly undersizing the coil. To obtain a more realistic sizing criterion, it was assumed that at some time during the winter the design load of the house, as determined by the ASHRAE 99% design temperature (16), would have to be met by the ground source heat pump with no assistance from the solar subsystem and with no electric resistance backup. Using this

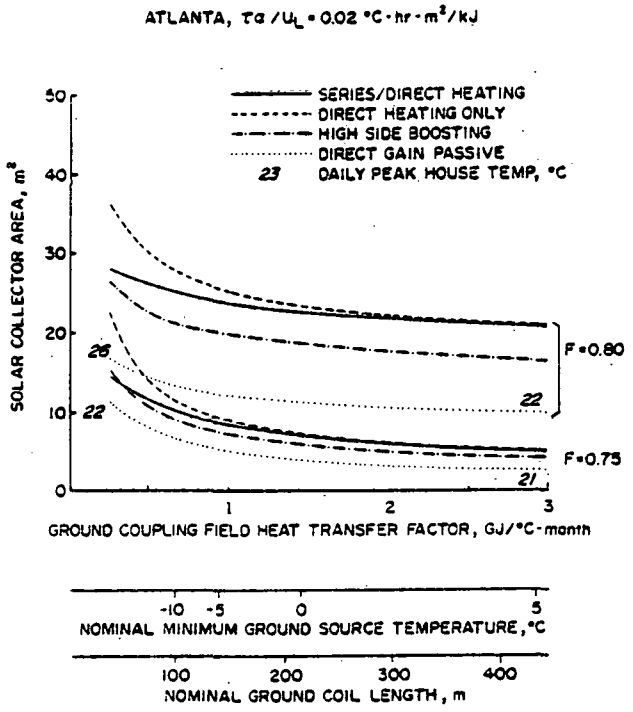

Figure 8. Solar Collector Areas and Ground Coupling Coil Capacities Required to Produce a Fraction F of Non-purchased Energy Use. Heat Pump Collector in Atlanta.

criterion, it is possible to calculate the temperature to which the ground coil must be drawn down in order to supply the required amount of heat to the heat pump. These minimum source temperatures are plotted along another horizontal axis on each of Figures 3 through 8. For the same reasons as given above, the adjective "nominal" is attached to these numbers as well. They are intended to be suggestive rather than definitive.

Estimates of the costs involved in installing ground coils have been obtained from a number of sources for depths in the range of 1 to 1.5 meters (17). Installed costs for the buried pipe coil, including excavation and backfill as well as the cost of the ~ 4 cm O.D. medium density polyethylene pipe, ranged from $4.07/m to $4.92/m.

Collector

It is seen from Figures 3 through 8 that an enhancement in system performance (as measured by the fraction of nonpurchased energy utilized by the system) results from the addition of solar collectors. It was desired to estimate how much one might reasonably pay for solar collectors, per unit area, to achieve this enchancement. A criterion that the incremental system cost should not exceed ten times the initial year's savings on energy costs was suggested (18) on the basis of payback, cash flow, and life-cycle costing considerations. Use of this criterion, together with an electricity cost of $0.05/kWh (18a), results in allowed costs for marginal additions to the solar subsystem, based on collector area, of $140/GJ of annual electrical energy savings. The results are shown in Table 4.

Table 4

Allowed Solar Subsystem Costs Based on Marginal Collector Area

City and Collector Type	Fraction of Non-Purchased Energy	Collector Area (m^2)	Marginal Electric Energy Savings (GJ_e/m^2-yr)	Allowed Cost for Marginal Collector Area ($/$m^2$)
Madison (b=2.0 GJ/°C-month)				
High Performance Collector	0.638	0		
($\tau\alpha/U_L$ = 0.04)			0.591	83
	0.70	12.1	0.392	55
	0.75	26.8	0.300	42
	0.80	46.0		
Heat Pump Collector	0.638	0		
($\tau\alpha/U_L$ = 0.02)			0.322	45
	0.70	22.2	0.184	26
	0.75	53.6		
Direct Gain Passive	0.638	0		
			0.567	79
	0.70	12.6		
New York (b=1.5 GJ/°C-month)				
High Performance Collector	0.663	0		
($\tau\alpha/U_L$ = 0.04)			0.516	72
	0.70	6.3	0.395	55
	0.75	17.4	0.303	42
	0.80	31.9		
Heat Pump Collector	0.663	0		
($\tau\alpha/U_L$ = 0.02)			0.332	46
	0.70	9.8	0.221	31
	0.75	29.7		
Direct Gain Passive	0.663	0		
			0.500	70
	0.70	6.5	0.399	56
	0.75	17.5		
Atlanta (b=1.0 GJ/°C-month)				
High Performance Collector	0.711	0		
($\tau\alpha/U_L$ = 0.04)			0.489	68
	0.75	4.6	0.407	57
	0.80	11.7		
Heat Pump Collector	0.711	0		
($\tau\alpha/U_L$ = 0.02)			0.317	44
	0.75	7.1	0.237	33
	0.80	19.3		
Direct Gain Passive	0.711	0		
			0.489	68
	0.75	4.6	0.413	58
	0.80	11.6		

The highest allowed costs of ~ $80/m^2 occur for the high performance collector in Madison. This is a low number by current standards. In order for it to be increased, however, one of the following would have to change in the direction indicated: a lower ground coupled heat pump COP than assumed here; a higher initial electricity cost; or a higher allowed ratio of initial system cost to first year's energy savings than ten. It should also be noted that cost constraints determined on a marginal basis may be more severe than if determined on a systemwide basis. That is, if other system components, such as the ground coil, can be made less expensive than required by system cost contraints, it may be possible to allocate some of the difference to the collectors.

RESEARCH AND DEVELOPMENT NEEDS

This paper has explored ground coupled solar heat pump systems in which the ground is used as a heat source (and sink for cooling) but not as a storage element. The most promising systems appear to be ground coupled heat pumps without additional solar input; ground coupled heat pumps with modest passive augmentation; and possibly ground coupled heat pumps with active solar augmentation, if high-performance collectors can be sold and installed at much lower cost than is generally the case now. The severe cost restriction on the solar components arises from the good projected performance of the ground-source heat pump and from the economic criterion used. Three areas of research and development whose pursuit is consistent with the results of this paper can be identified. They are:

1. Development of ground coupled heat pump technology and design tools.
2. Development of low-cost high-performance collectors.
3. Continued investigation of the merits of ground coupled solar heat pump configurations in which the ground is used as a storage element and not as source/sink only.

SUMMARY

The following statements summarize the results of the study:

1. With the high performance collector there was no benefit to be gained by passing the collected solar energy through the heat pump in any of the three cities studied. That is, when given the choice between operating in the series mode at any source temperature below 40°C, and operating in the direct heating mode at any temperature at or above 40°C, the optimization procedure always selected direct heating at 40°C.
2. Direct-gain passive with night insulation provided about the same benefit per unit collector area as the high performance collector, for aperture areas below that imposed by the requirement that the building not overheat.
3. When the heat pump collector was used, both the series and boosting modes provided better performance than direct heating, with the improvement increasing with increasing latitude. However, the performance of the heat pump collector (in its best mode) fell increasingly behind that of the direct heating collector (in its best mode), as one went further north. The allowed cost for the heat pump collector was about one-half (in Madison) to two-thirds (in Atlanta) that of the high performance collector or the direct-gain passive.
4. The allowed costs for all the collectors were low by current standards, the highest values being approximately $80/m^2 for the first 12 m^2 of high performance collector or direct gain passive in Madison. These numbers resulted from an allowance of $140/GJ of annual electricity savings, and will scale linearly with changes in this assumption.

REFERENCES

1 Bose, J. E., "Design and Field Testing of Solar Assisted Earth Coils", Annual Report, U.S. DOE Contract EM-78--S-01-4257, Oklahoma State University, 1979, p. 17; a., p. 15.

2 Andrews J. W., "Optimization of Solar Assisted Heat Pump Systems Via a Simple Analytic Approach", Proceedings of Systems Simulation and Economic Analysis Conference, San Diego, January 23-25, 1980, SERI/TP-351-431, p. 361.

3 Duffie, J. A. and Beckman, W. A., Solar Energy Thermal Processes, Wiley, New York, 1974, pp. 138-151.

4 Klein, S. A., Beckman, W. A., and Duffie, J. A., "A Design Procedure for Solar Heating Systems", Solar Energy, Vol. 18, 1975, pp. 123-4.

5 Wynn, C. B. and Johnson, G. R., "Solar Energy Analysis Programs for Programmable Handheld Calculators", SEEC-TR-99, 1977, Solar Environmental Engineering Inc.

6 Lewis, D. and Fuller, W., "Restraint in Sizing Direct Gain Systems", Solar Age, Vol. 1, No. 12, December 1979, pp. 28-32.

7 Kahan, W. and Estes, R. C., "Optimization and Comparison Strategies for Solar Energy Systems", ASME Publication 79-WA/SOL-26, 1979.

8 Granryd, E., "Experience in Ground Source Heat Pump Systems in Scandinavia", Proceedings of the Workshop Performance of Heat Pump Systems, Aachen, West Germany, May 8-9, 1980 (Sponsored by the German Section of ISES).

9 Kush, E. A., "Experimental Performance Study of a Series Solar Heat Pump", Proceedings of the ISES International Congress, Atlanta, May 1979, p. 812

10 Dollars, W., et al., "Development of Marketable Solar Assisted Heat Pumps-Residential Design Review", Lennox Industries Inc., Carrolton, Texas, 1978, p. 1-3. Report prepared under U.S. DOE Contract EG-78-C-03-1720.

11 Proceedings of the Annual DOE Active Solar Heating and Cooling Contractors' Review Meeting, Section 4 (Solar Heat Pump Systems), CONF 800340, March 1980.

12 Labs, K., "Underground Building Climate", Solar Age, Vol. 4, No. 10. Oct. 1979, pp. 44-50.

13 ASHRAE Standard 70-75, "Energy Conservation in New Building Design", New York, 1975.

14 Bessler, W. F. and Hwang, B. C., "Solar Assisted Heat Pumps for Residential Use," ASHRAE Journal, Sept. 1980, p. 39.

15 Andrews, J. W. and Metz, P. D., "Computer Simulation of Ground Coupled Storage in a Series Solar Assisted Heat Pump System," Proceedings of the ISES International Congress, Atlanta, May 1979, p. 791.

16 ASHRAE Handbook of Fundamentals, 1977, p. 23.3.

17 E-Tech, Inc., "Solar Assisted Heat Pump Field Performance Evaluation" Final Report, Contract No. DE-AC03-79SF10549 (Draft) quotes in Table III a maximum installation cost of $1.50/ft ($4.92/m). E. Granryd, Ref. 8, quoted SKR 7400 for ~400m installed, or $4.40/m at SKR 4.20 per dollar. P. Metz, Brookhaven National Laboratory, received bids of $1.00 and $1.10/ft to excavate, install, and backfill 500 ft of pipe at 4 ft depth (personal communication, 1980). Adding the $0.24/ft which the pipe itself cost yields a cost of $1.24 to $1.34/ft ($4.07 to $4.40/m). These quotes are all for ~4cm (~1.5 in.) O.D. medium-density polyethylene pipe, and should be viewed as a contractor's installed cost. Contractor overhead and profit should be added to obtain an installed cost to the customer. J. E. Bose, Ref. 1, p. 18 quotes an installed cost of $2.00 to $3.00/ft ($6.56 to $9.84/m) for the more expensive 4 in. (10 cm) O.D. PVC pipe.

18 Andrews, J. W., "Cost/Performance Goals for Combined Solar Heat Pump Systems", BNL 51259, 1980, Brookhaven National Laboratory; a., p. 14.

19 Hall, I. J., et al., "Generation of Typical Meteorological Years for 26 SOLMET Stations", SAND 78-1601, 1978, Sandia Laboratories.

20 Klein, S. W., et al., "TRNSYS A Transient Simulation Program", University of Wisconsin Engineering Experiment Station, Report 38, 1976.

21 Liu, B. Y. H. and Jordan, R. C., "The Interrelationship and Characteristic Distribution of Direct, Diffuse, and Total Solar Radiation", Solar Energy, Vol. 4, 1960, pp 1-19.

APPENDIX: DERIVATION OF EQUATION 1.

Probability Distribution of Insolation

Using Typical Meteorological Year (TMY) weather data (19) and the solar radiation processor subroutine in TRNSYS (20) which converts total horizontal insolation to total insolation on a tilted surface according to the method of Liu and Jordan (21), the number of hours in which tilted-surface incident radiation values fell into each of six classes was determined. Table 5 shows these results for Madison, New York, and Nashville (Nashville being the closest TMY city to Atlanta). On the basis of these data, it was decided to use a uniform probability distribution of insolation between the values 0 and 3410 kJ/m^2-hr (300 Btu/ft^2-hr). The principal deviation of the data from this assumption is the excess of hours in the first bin (1 to 682 kJ/m^2-hr). Since this bin has the lowest insolation per hour, any deviation of this bin from the average will have the least effect on results. Moreover, when this bin is more finely divided, it is found to skew towards its lower limit. The excess of insolation in this bin was 3% of the total annual insolation in Madison and Nashville, and 4% in New York.

The other deviation from uniformity is the fact Bin 5 (2729 to 3410 kJ/m^2-hr) tends to have fewer hours than Bins 2, 3, and 4. This is partially compensated by the existence of hours above 3410, expecially in Madison. Although it would be possible to refine the analysis by departing from uniformity or by varying the upper limit of the distribution either month by month or from city to city, in the interest of simplicity it was decided to use a uniform distribution running from 0 to 3410 kJ/m^2-hr in all cases.

Total Collectable Insolation

Writing the collector efficiency as

$$\eta = F_R\tau\alpha - F_R U_L (T - T_a)/I \qquad (15)$$

and letting the time in hours that the received insolation on a tilted surface falls between I and I + dI (given that $0<I<I_m$) be $(h/I_m)dI$, where h is the number of hours with sun, the energy E_c collected for insolation values between I and I + dI is

$$dE_c = A\,(h/I_m)\,I\eta\,dI$$

$$= A\,(h/I_m)\,I\,dI[F_R\tau\alpha - F_R U_L (T-T_a)/I] \qquad (16)$$

Table 5

Frequency Distribution of Total Insolation Rates on Tilted Surface

City	Insolation Rate (kJ/m^2-hr)					
	1 to 682	683 to 1364	1365 to 2046	2047 to 2728	2729 to 3410	>3410
Madison	1289	733	575	548	511	95
New York	1480	674	637	624	352	15
Nashville	1305	732	632	701	462	14

In order to find the total collected energy E_c one integrates (16) from the minimum I for which collection is possible up to I_m.

This minimum insolation is just the value of I for which η equals zero, namely $(T-T_a)\ U_L\ /\tau\alpha$. Then

$$E_c = \frac{Ah}{I_m} \int_{(T-T_a)\ U_L/\tau\alpha}^{I_m} [I\ F_R\ \tau\alpha - F_R\ U_L\ (T-T_a)]\ dI \qquad (17)$$

$$= \frac{Ah F_R \tau\alpha}{2I_m} \left[I_m - \frac{U_L(T-T_a)}{\tau\alpha} \right]^2$$

If we further note that the total received insolation is given by

$$S = \int_0^{I_m} I\ (h/I_m)dI = hI_m/2 \qquad (18)$$

and that the maximum stagnation temperature of the collector is

$$T_m = T_a + I_m\tau\alpha/U_L \qquad (19)$$

then

$$E_c = SAF_R\ \tau\alpha \left(\frac{T_m - T}{T_m - T_a} \right)^2 \qquad (20)$$

which is the same as (1).